Bilateral, Difunctional Nanosphere Aggregates and Their Assembly Mediated by Polymer Chains

S. M. Barber,[†] P. J. Costanzo,[‡] N. W. Moore,[†] T. E. Patten,[‡] K. S. Lancaster,[‡] C. B. Lebrilla,[‡] and T. L. Kuhl*[,†]

Department of Chemistry and Department of Chemical Engineering and Materials Science, University of California—Davis, One Shields Ave., Davis, California 95616

Received: October 22, 2005; In Final Form: January 30, 2006

We have developed an efficient method for producing difunctional, bilateral nanospheres. A monolayer of nanoparticles was prepared followed by deposition of a thin layer of metal. By varying the base particle and metal deposited, bilateral nanoparticles were formed. The different regions of the nanoparticles were selectively functionalized with polymer linkers containing specific terminal groups, thereby creating bilateral, difunctional nanoparticles. Subsequent covalent cross-linking of different nanoparticles enabled the formation of stable architectures with programmed hierarchy and controlled chemical composition.

1. Introduction

The future success of nanotechnology will rely on the assembly of nanoscale building blocks to create highly specific, anisotropically structured materials with embedded functionality and physical properties. These engineered materials can be used to create materials tailored for highly specific applications. Recently, there has been much work in the preparation of self-assembling aggregates. Many different groups have used Langmuir−Blodgett approaches,[1−3] controlled solvent evaporation,[4,5] biological or polymeric templating,[6−10] and polymer and surfactant-assisted aggregation to prepare self-assembled aggregates.[11,12] However, a limitation of using symmetric components is that the final material will also be symmetric.

Progress has been made toward the removal of symmetry in nano-objects. For example, the selective growth of PbSe nanoparticles upon the tips of CdSe nanorods[13] is plausible because of the different reactivity of the crystal faces.[14−19] The primary goal of our work is to control the arrangement and interactions of asymmetric, spherical particles through selective surface functionalization. By controlling the anisotropy and composition of the particles, a variety of symmetric or asymmetric materials can be prepared from a small number of building blocks. Moreover, different particle and surface materials can be utilized to generate particles and aggregates for specific applications, e.g., designer surface layers, catalysts, assemblies for ELISA-type assays, optical waveguide materials, or novel three-dimensional materials (Figure 1).

In this work we report on methods to specifically surface pattern and self-assemble nanospheres into hierarchical structures with a defined orientation. We describe a pathway to circumvent the limitations of the symmetric assembly of spheres. We present an engineering framework to tailor their assembly using polymer chains to bind specifically to surface-patterned regions of the nanospheres and act as cross-linkers. Furthermore, this approach can be applied to nonspherical objects, i.e., rods, tetrapods, and cubes.

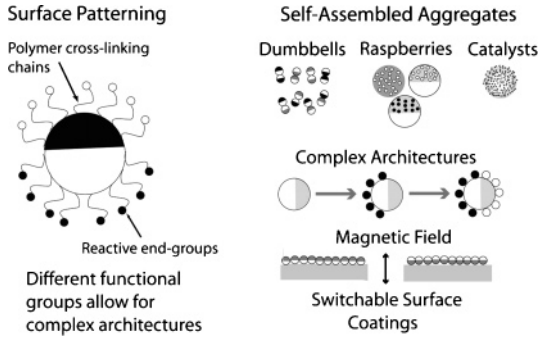

Figure 1. Schematic of the bottom-up assembly of bilateral, difunctional particles and aggregates.

2. Experimental Section

2.1. Preparation and Characterization of Polymer Linkers. All reagents were ACS grade and purchased from Sigma-Aldrich. The general set of reactions for synthesizing functional polymer cross-linking chains is depicted in Scheme 1. First, 18-crown-6 (0.95 g, 3.6 mmol), dry THF (30 mL), and acetonitrile (125 μL, 2.40 mmol) were mixed with a solution of potassium naphthalide (2.4 mL, 1 M in THF) to generate an initiator. Next, ethylene oxide (15 mL, 301 mmol) was introduced into the reaction flask via a cooled syringe, and the reaction was stirred at room temperature for 48 h. The growing alkoxide chain end was then terminated by addition of methanesulfonyl chloride (0.37 mL, 4.8 mmol). At this stage, the reaction could be treated with either thioacetic acid (0.52 mL, 10.0 mmol) or NaN_3 (470 mg, 7.2 mmol) to install either a mercapto or amino functionality at the ω-chain end. The synthesis of the poly(ethylene glycol) (PEG) linker containing a siloxyl ether linkage will be reported elsewhere.[25] The polymer linkers used in this study had a M_n of about 2800 g/mol with a polydispersity of 1.13.

IR samples were prepared as neat films upon a NaCl plate, and analysis was conducted on a Matteson Galaxy Series FTIR 3000. Number average molecular weights (M_n) and polydispersities (PDI) were determined using gel-permeation chromatography in THF at 25 °C and a flow rate of 1.00 mL min^{-1}.

* Corresponding author. Phone: (530) 754-5911. Fax: (530) 752-1031. E-mail: tlkuhl@ucdavis.edu.
[†] Department of Chemical Engineering and Materials Science.
[‡] Department of Chemistry.

10.1021/jp0560617 CCC: $33.50
Published on Web 03/09/2006

SCHEME 1: Synthetic Route for the Preparation of PEG Linkers[a]

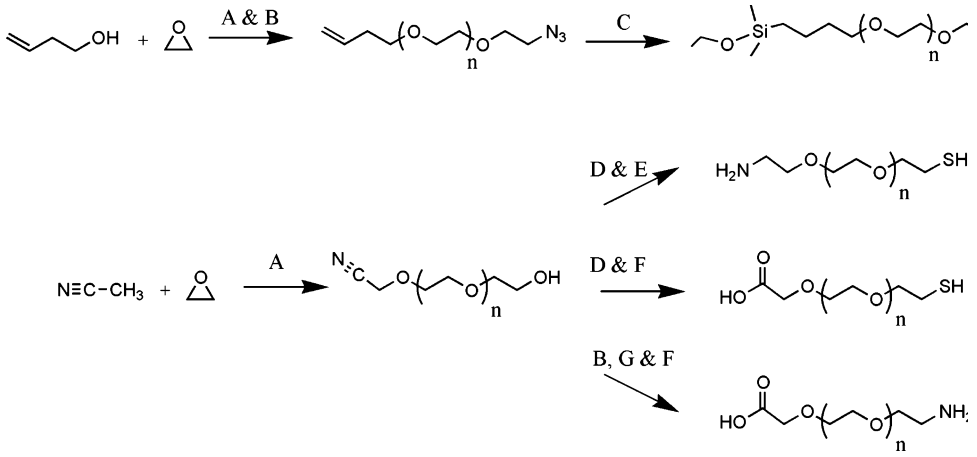

[a] Conditions: (A) K/naphthalenide; (B) MsCl, Et_3N then NaN_3; (C) $HSi(CH_3)_2OEt$, [Pt]; (D) MsCl, Et_3N then CH_3COSH; (E) $LiAlH_4$, THF; (F) HCl, H_2O, Δ; (G) PPh_3, H_3PO_4

Three Polymer Standards Service columns (100 Å, 1000 Å, and linear) were connected in series to a Thermoseparation Products P-100 isocratic pump, autosampler, column oven, and Knauer refractive index detector. Calibration was preformed using polystyrene standards (Polymer Standards Service, $M_p = 400-1\,000\,000$; $M_w/M_n < 1.10$. Mass spectra were recorded on an external source HiResMALDI (IonSpec Corp., Irvine, CA) equipped with a 4.7 T magnet. The HiResMALDI was equipped with an LSI 337-nm nitrogen laser. Mass spectra were also recorded on a Proflex III MALDI-FT (Bruker-Daltonics, Billerica, MA) with a 337-nm nitrogen laser. The matrix used was 2,5-dihydroxybenzoic acid (5 mg/100 μL in ethanol).

2.2. Preparation and Characterization of Bilateral Nanospheres and Aggregates. SiO_2, carboxylate-functionalized polystyrene, and nonfunctionalized polystyrene particles were purchased from Polysciences, Inc. and Bangs Laboratories, Inc. Beads were cleaned prior to use following manufacturer's guidelines. Typically, a monolayer of particles was prepared on a substrate (glass, mica, or silicon) by either slow evaporation of solvent or by using Langmuir−Blodgett techniques. Next, the nanospheres were made anisotropic by coating with Au or Ag layers. The metal layers were evaporated upon the substrate-supported particles, either by thermal evaporation or sputter coating.[20−24] The metal-coated particles were released from the substrate by either sonication or physically scraping the particles from the surface. The morphology of the metal surface coating (e.g. Au or Ag) was varied by deposition and thickness of adhesion layers (e.g., chromium) and manipulating the deposition rate, the substrate temperature, and the operating pressure in the deposition chamber. The bilateral nanospheres were then selectively functionalized with PEG chains by incubating the desired PEG with bilateral nanospheres in ethanol for a minimum of 8 h. After rinsing to remove nonreacted material, complementary nanospheres dispersed in ethanol were added to construct nanospheres aggregates. The mixture was incubated for another 8 h and subsequently rinsed. For SEM imaging, dilute droplets of the ethanol solution containing PEG cross-linked aggregates were placed on copper grids. Digital SEM images were obtained using an FEI XL-30 SFEG operated at 5 kV.

3. Results and Discussion

3.1. Polymer Linkers. To link anisotropic spheres together into prescribed hierarchical aggregates, poly(ethylene glycol) (PEG) linkers of differing chain lengths (average molecular weights ranging from 10^2 to 10^5 g/mol) and chain end functionalities were prepared using living anionic ethylene oxide polymerization coupled with high-yielding organic functional group transformations (Scheme 1). The cyano chain end of the α-cyano-ω-thioacetate PEG was transformed into either an amine or carboxylic acid functional group. Confirmation of this conversion was obtained through MALDI-TOF mass spectra, FTIR spectra, and ninhydrin tests.

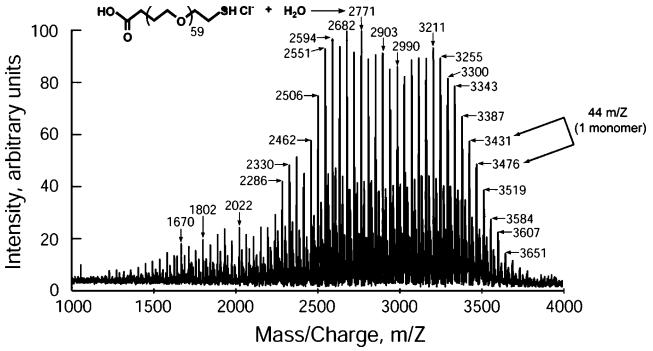

Figure 2. MALDI-FT spectrum of α-carboxy-ω-mercapto PEG with the chemical structure of the expected molecule of $m/z = 2771$ g/mol shown.

Figure 2 shows the MALDI-FT spectrum of α-carboxy-ω-thiol PEG. The spectrum shows a continuous distribution of chains with one major and one minor series. The interval between isotopic clusters of signals is 44 *m/z*, which corresponds to the repeat unit of PEG. Examination of the signal cluster at 2771 *m/z*, for example, showed a signal at 2769 *m/z*, corresponding to the empirical formula of $C_{122}H_{246}O_{62}ClS$, with an isotopic distribution in which the highest intensity signal is 2771 *m/z*. A calculated isotopic distribution pattern for this empirical formula (2769 at 70.1%, 2770 at 96.5%, 2771 at 100.0%, 2772 at 77.4%, 2773 at 47.1%, 2774 at 23.8%, 2775 at 10.3%, and 2776 at 3.8%) matched the intensities of the experimentally measured cluster of signals. This particular formula corresponded to a PEG chain structure of 59 repeat units, a $-CH_2-CO_2H$ α-chain end structure, and a $-CH_2CH_2SH$ ω-chain end structure. Additionally, the chain was co-ionized with a proton and a molecule of $H_3O^+Cl^-$, presumably residual acid from the hydrolysis step. The minor series corresponded to ionization of the chains with an additional molecule of H_2O. Ninhydrin test of this product yielded a negative result, which was expected because the cyano chain end was hydrolyzed completely to a carboxylic acid functional group. An IR spectrum of the starting

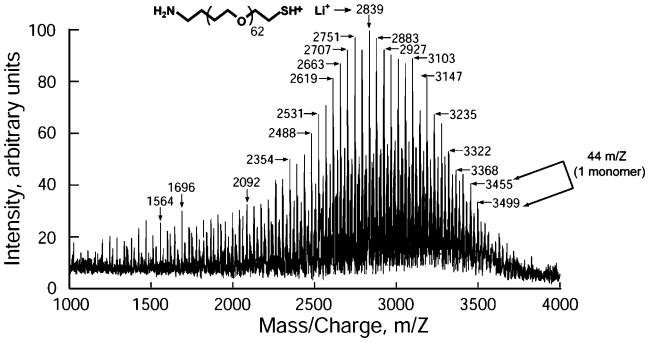

Figure 3. MALDI-FT spectrum of α-amino-ω-mercapto PEG with the chemical structure of the expected molecule of $m/z = 2839$ g/mol shown.

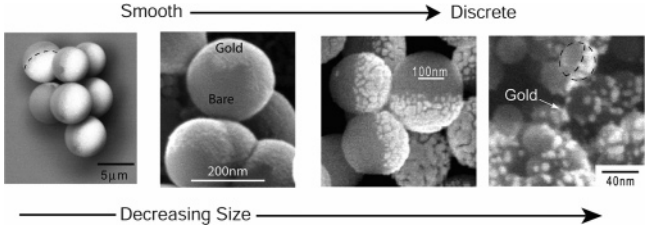

Figure 4. SEM imaging of anisotropic spheres. Particle aggregation occurs upon solvent evaporation during sample preparation. Composition of nanoparticle for first image is polystyrene with Ag. Composition of nanoparticles for last three images is SiO_2 with Au.

α-cyano-ω-thioacetate PEG showed signals at 1984 and 1702 nm^{-1}, consistent with the presence of nitrile and thioester functional groups, respectively. After hydrolysis with HCl/H_2O, an IR spectrum showed signals at 3204, 2906, and 1685 nm^{-1}, corresponding to the presence of carboxylic acid and thiol functional groups.

Figure 3 shows the MALDI-FT spectrum of α-amino-ω-thiol PEG. The spectrum showed a continuous distribution of chains with one major and one minor series. The interval between isotopic clusters of signals is again 44 *m/z*, which corresponds to the repeat unit of PEG. Examination of the signal cluster at 2839 *m/z*, for example, revealed that it was a convolution of isotopic patterns for two species of empirical formulas $C_{128}H_{259}O_{62}LiNS$ and $C_{128}H_{257}O_{62}LiNS$. These formulas corresponded to a PEG chain structure of 62 repeat units, a $-CH_2CH_2NH_2$ α-chain end structure, and a $-CH_2CH_2SH$ ω-chain end structure and to a PEG chain structure of 61 repeat units, a $-CH_2CH_2NH_2$ α-chain end structure, and a $-CH_2CH_2SC{=}OCH_3$ ω-chain end structure, respectively. Both chains were co-ionized with a lithium ion, presumably residual from the reduction step. The minor series corresponded to ionization of the chains with an additional molecule of H_2O and of a small amount of dimer derived from the PEG chains with the $-CH_2CH_2SH$ ω-chain end structure. The ninhydrin test of this product yielded a positive result, which confirms the presence of the amino functional group. An IR spectrum of the product from the reduction of α-cyano-ω-thioacetate PEG with $LiAlH_4$ showed signals at 3204 and 2906 nm^{-1}, corresponding to the presence of amino and thiol functional groups. Signals for the thioacetate structere were not observed, even though the mass spectrum clearly indicates the incomplete hydrolysis of this group to the thiol chain end group.

3.2. Bilateral Nanospheres. As shown in Figure 4 (from left to right, respectively), the quality of metal coatings may be straightforwardly tuned from smooth, highly reflective continuous layers to discrete nanoislands. This ability to tailor the morphology of the coating affords another means for surface patterning. We next covalently grafted functionalized PEG chains onto the surface coatings and investigated procedures for the assembly and cross-linking of such spheres into structures such as "dumbbells" (two similar sized hemispherically attached spheres) and "raspberries"[26] (smaller particles of one type attached to another particle). The surface patterning and functionalization enables us to specifically link particles together in predetermined orientations.

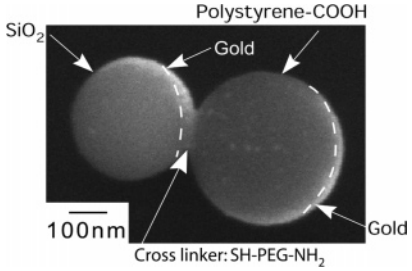

Figure 5. SEM image of the rare dumbbell assembly of two complimentary particles. Composition of particles: (left) 400-nm SiO_2 plated with Au and functionalized with HS-PEG-NH_2, (right) 510-nm COOH-functionalized polystyrene plated with Au. The reaction between the PEG-NH_2 and COOH surface covalently cross-links the particles together in a "dumbbell" configuration.

3.3. Controlled Aggregate Assembly. We now present two prototypical structures, the dumbbell and raspberry configurations. Both "half-raspberry" and "whole-raspberry" configurations were easily obtained, whereas the dumbbell configuration was rarely produced. Figure 5 illustrates the rarely observed dumbbell architecture. The left particle is a 400-nm SiO_2 nanosphere plated with Au and treated with an amine-functionalized thiol PEG chain (HS-PEG-NH_2), creating a thiol−gold linkage to the surface. The right particle is a 510-nm polystyrene nanosphere with a surface containing carboxylic acid functional groups. In this case, the Au metal coating masks a portion of the particle. The two particle types were then mixed together. The PEG chains linked to the SiO_2 particles extends the amine ligand in the solution, which allows it to react with the carboxylic acid of the polystyrene particle surface, thereby creating the dumbbell structure (Figure 5).[31]

Figure 6 shows structures of the half-raspberry and whole-raspberry morphology comprised of different types of nanoparticles. Figure 6A illustrates a cross-linking reaction between 400-nm SiO_2 particles and 5-μm polystyrene particles. The polystyrene particles were hemispherically coated with Ag and functionalized with HS-PEG-NH_2. The SiO_2 particles were hemispherically coated with Au and functionalized with carboxy-terminated thiol PEG (HS-PEG-COOH). In solution the PEG-NH_2-functionalized polystyrene particles reacted with the PEG-COOH-functionalized particles to form the aggregate structure. It is interesting to note that the structure of Figure 6A was more readily formed than the dumbbell structure of Figure 5. One would expect that the formation of a bond between the ends of two polymer chains would be less likely than that of a single polymer chain finding a functionalized surface.

Figure 6B illustrates the whole-raspberry morphology utilizing 14-nm gold nanoparticles[27,28] and 500-nm polystyrene particles. The gold nanoparticles were treated with an HS-PEG-NH_2 and the polystyrene nanoparticles contained carboxylic acid moieties already built into the surface. Similar to the dumbbell example (Figure 5), here the PEG-NH_2 needed to only interact with a carboxylic acid surface site to create a cross-link.

3.4. Polymer Chain Properties and Cross-Bridge Formation. The rate at which the complementary pairing will occur

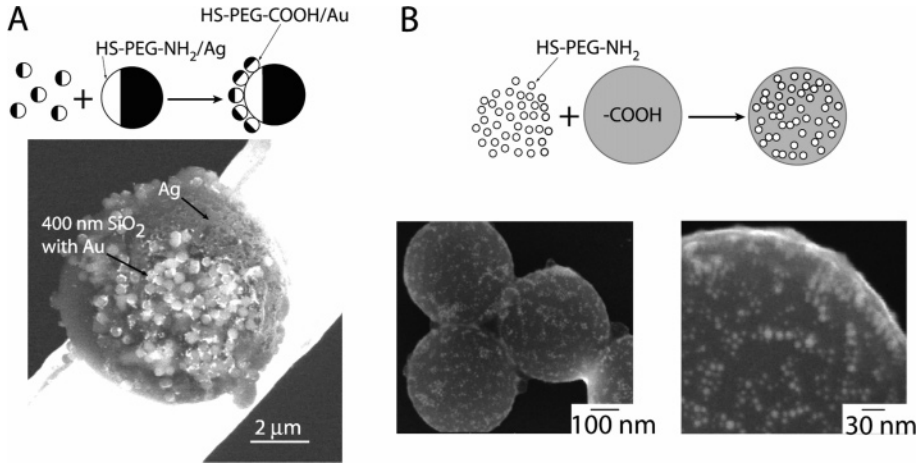

Figure 6. (A) SEM image of a half-raspberry assembly of two complimentary particles. The large particle is 5-μm polystyrene plated with Ag and functionalized with HS-PEG-NH_2. The small particles are 400-nm SiO_2 plated with Au that have been functionalized with HS-PEG-COOH. (B) SEM image of whole-raspberry assembly of complimentary particles. Composition of particles: 14-nm Au functionalized with HS-PEG-NH_2 and 500-nm COOH-functionalized polystyrene.

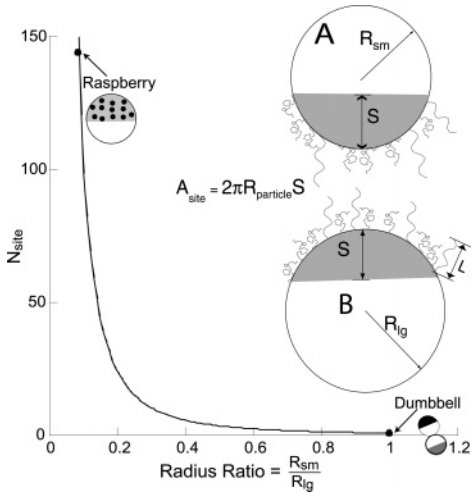

Figure 7. A plot of the number of interaction sites, N_{site}, as a function of the radius ratio of two interacting particles (where the length of the polymer linker is negligible). Filled data points refer to the results in Figures 5 and 6A. (Inset) Drawing illustrating the relationships between R (particle radius), S (functionalized portion of the particle), A_{site} (interaction site area), and L (length of the polymer chain). L is determined by the composition and molecular weight of the polymer chain and may be expressed as a fraction of the radius of the particle, R.

is limited by the number of polymer chains on the surface of the particle, i.e., the effective surface concentration of polymer chains, and the spatial exploration of the reactive chain end. The polymer energy potential determines this sampling rate, and hence the kinetics of complimentary pairing between two surfaces in close proximity. Once a particle is within a distance less than the full extension of a polymer chain, L, a complementary bond can form (Figure 7, inset). However, there is a higher energy cost for the polymer chain to stretch to an extension greater than its equilibrium extension. This energy cost translates into a shorter time that the chain will spend in a given stretched configuration. As a result, the polymer cross-linker provides additional means to tune the rate of particle−particle pairing, i.e., kinetics, as well as the probability of binding. Assuming that the polymer surface adsorption is low, i.e., that there is no nearest neighbor overlap, end-grafted polymers attached to a surface will adopt a "mushroom" configuration, where the area per polymer chain on the surface can be approximated by the square of the characteristic Flory radius, R_F^2.[30] The number of grafted chains per particle can be estimated from the area when two particles are in contact and the length of the polymer cross linker. For example, with a 3000-g/mol PEG chain, the number of chains on the functionalized portion of the 400 nm particle is estimated to be 750 (e.g., Figure 5, inset of Figure 7). [If one approximates the area per polymer chain on the surface as πR_F^2, then the estimate for the number of cross-bridges would be 658. In this case the factor of π in the polymer chain area decreases the number of bonds by approximately 70%.] Likewise, the area per carboxylic acid group on the surface of the 510-nm polystyrene particles is 1.28 nm^2 (Interfacial Dynamics Corp.), so there are approximately 1.4×10^4 carboxylic acid sites available to which the complementary polymer chain ends may react. When one makes similar assumptions for the case of the half-raspberries, there are again about 950 potential polymer chain cross-bridges. Moreover, in this case complementary chains on the two particles must meet and react to form the cross-link. In the case of the much smaller PEG-NH_2-functionalized gold nanoparticles (14 nm), less than 25 polymer chains could potentially form bonds with the complementary COOH groups on the 510-nm polystyrene particles, yet these composite aggregates formed easily. In these examples, the number of potential cross-bridges is insufficient to explain the difference in efficacy of aggregate formation. While there are other parameters, e.g., Brownian motion, hydrodynamic effects, particle settling time, that have a hand in determining the discrete rate and efficiency of particle binding, on the basis of the similarity of our conditions in the above cases, we hypothesize that a critical factor not typically considered in predicting assembly efficiency may be the radius ratio between the particles. Statistically, the likelihood of particles A and B reacting will increase with the number of possible interaction sites for A on B. The number of interaction sites, N_{site}, is simply the ratio of the available binding areas on the two particles. For example, the preparation of dumbbell structures was highly improbable, as the two particles only possessed one point of contact, similar to two billiard balls colliding. Conversely, the preparation of raspberries was facile due to the increased number of possible areas of interaction available on a large particle for smaller particles, e.g., marbles lying on a table. The effects of the radius ratio and the particle−particle interaction area may be expressed in a relationship to quantify the maximum number of interaction sites, N_{site}, available for binding between two given particles and the length

of the polymer cross-linker, L. The general form of N_{site} for two spheres of radius R is given by $N_{site} = (4\pi/4\pi)\,(R_{lg} + L_{lg}/R_{sm} + L_{sm})^2$. In the case of surface patterning, the functionalized zone of the sphere, $2\pi RS$, is used, as illustrated in Figure 7: $N_{site} = (2\pi R_{lg}/2\pi R_{sm})\,(S_{lg} + L_{lg}/S_{sm} + L_{sm})$. When the length of the chain is much shorter than the particle radius or the polymer chains are on the order of the size of the particles, the number of interaction sites may be approximated as $N_{site} \cong (R_{lg}/R_{sm})^2$. As shown in Figure 7, as the radius ratio decreases, the greater the likelihood that a given small particle will bind with a large particle. This simple analysis is in agreement with our anecdotal evidence (Figures 5 and 6) and suggests that the number of interaction sites accurately depicts the difficulty of particle−particle bond formation.

In summary, we have coupled synthesis and self-assembly to produce, in situ, complex higher order structures of nanoparticle aggregates. We have developed anisotropic nanoparticles and chain end reactive polymers to program the nanoparticle surface for assembly. We have proposed a method to determine efficiency of binding of a given pair of particles by looking at the number of interaction areas available on the complementary particle. To further modulate the efficiency of pairing, we suggest future studies of the effect of tailoring the polymer cross-linker properties. Control of the self-assembly process is required to consistently yield desired hierarchical structures.

Acknowledgment. The authors thank Mike Dunlap for SEM imaging and Frank Osterloh and Hiroki Hiramatsu for the synthesis of gold nanoparticles. The authors would like to acknowledge Anthony Delacruz for his assistance with establishing protocols. The authors would also like to acknowledge the work of Emily Conley and Yelena Semenov during their participation in the CPIMA REU program (DMR-9808677). This work was supported by NSF NER DMII-0404457 and Grant Number T32-GM08799 from NIH-NIGMS. Its contents are solely the responsibility of the authors and do not necessarily represent the official views of the NIGMS or NIH.

References and Notes

(1) Burghard, M.; Philipp, G.; Roth, S.; von Klitzing, R.; Pugin, R.; Schmid, G. *Adv. Mater.* **1998**, *10*, 842.

(2) Heath, J. R.; Knobler, C. M.; Leff, D. V. *J. Phys. Chem. B* **1997**, *101*, 198.

(3) Nakahama, K.; Kawaguchi, H.; Fujimoto, K. *Langmuir* **2000**, *16*, 7882−7886.

(4) Wang, Z. L. *Adv. Mater.* **1998**, *10*, 13.

(5) Micheletto, R.; Fukuda, H.; Ohtsu, M. *Langmuir* **1995**, *11*, 3333−3336.

(6) Claridge, S. A.; Goh, S. L.; Frechet, J. M. J.; Williams, S. C.; Micheel, C. M.; Alivisatos, A. P. *Chem. Mater.* **2005**, *17*, 1628−1635.

(7) Boal, A. K.; Ilhan, F.; DeRouchey, J.; Thurn-Albrecht, T.; Russell, T. P.; Rotello, V. M. *Nature* **2000**, *404*, 746.

(8) Wang, S.; Yan, J.; Chen, L. *Mater. Lett.* **2005**, *59*, 1383.

(9) Costanzo, P. J.; Patten, T. E.; Seery, T. A. P. *Chem. Mater.* **2004**, *16*, 1775.

(10) Hiddessen, A. L.; Rodgers, S. D.; Weitz, D. A.; Hammer, D. A. *Langmuir* **2000**, *16*, 9744−9753.

(11) Ramos, L.; Lubensky, T. C.; Dan, N.; Nelson, P.; Weitz, D. A. *Science* **1999**, *286*, 2325−2328.

(12) Ramos, L.; Weitz, D. A. *Langmuir* **2001**, *17*, 2275−2277.

(13) Kudera, S.; Carbone, L.; Casula, M. F.; Cingolani, R.; Falqui, A.; Snoeck, E.; Parak, W. J.; Manna, L. *Nano Lett.* **2005**, *5*, 445.

(14) Puzder, A.; Williamson, A. J.; Zaitseva, N.; Galli, G.; Manna, L.; Alivisatos, A. P. *Nano Lett.* **2004**, *4*, 2361.

(15) Manna, L. S.; E. C.; Alivisatos, A. P. *J. Am. Chem. Soc.* **2000**, *122*, 12700.

(16) Milliron, D. J.; Huges, S. M.; Cui, Y.; Manna, L.; Li, J. B.; Wang, L. W.; Alivisatos, A. P. *Nature* **2004**, *430*, 190.

(17) Mokari, T.; Rothenberg, E.; Popov, I.; Costi, R.; Banin, U. *Science* **2004**, *304*, 1787.

(18) Peng, Z. A.; Peng, X. G. *J. Am. Chem. Soc.* **2001**, *123*, 1389.

(19) Peng, Z. A.; Peng, X. G. *J. Am. Chem. Soc.* **2002**, *124*, 3343.

(20) Haynes, C. L.; Van Duyne, R. P. *J. Phys. Chem. B* **2001**, *105*, 5599−5611.

(21) Haynes, C. L.; McFarland, A. D.; Smith, M. T.; Hulteen, J. C.; Van Duyne, R. P. *J. Phys. Chem. B* **2002**, *106*, 1898−1902.

(22) Whitesides, G. M.; Boncheva, M. *Proc. Natl. Acad. Sci. U.S.A.* **2002**, *99*, 4769−4774.

(23) Takei, H.; Shimizu, N. *Langmuir* **1997**, *13*, 1865−1868.

(24) Qin, D.; Xia, Y. N.; Xu, B.; Yang, H.; Zhu, C.; Whitesides, G. M. *Adv. Mater.* **1999**, *11*, 1433−1437.

(25) Costanzo, P. J.; Dan, N.; Patten, T. E. Manuscript in preparation.

(26) Storhoff, J. J.; Mirkin, C. A. *Chem. Rev.* **1999**, *99*, 1849−1862.

(27) Osterloh, F.; Hiramatsu, H.; Porter, R.; Guo, T. *Langmuir* **2004**, *20*, 5553−5558.

(28) Hiramatsu, H.; Osterloh, F. E. *Chem. Mater.* **2004**, *16*, 2509−2511.

(29) Jeppesen, C.; Wong, J. Y.; Kuhl, T. L.; Israelachvili, J. N.; Mullah, N.; Zalipsky, S.; Marques, C. M. *Science* **2001**, *293*, 465−468.

(30) Kuhl, T. L.; Leckband, D. E.; Lasic, D. D.; Israelachvili, J. N. *Biophys. J.* **1994**, *66*, 1479−1488.

(31) The explicit orientation of the gold-coated portion of the SiO_2 particle relative to that of the non-gold-coated portion of the poly(styrene) particle suggests the desired interaction between the amine groups of the polymer chain with the surface carboxyl groups. In ethanol, the pH of carboxylic acid is approximately 5 while the SiO_2 surface (silanol) pH is 6.7. The pH of a protonated amine is approximately 10. Therefore, it is ∼100 times more likely that an amine will deprotonate a carboxylic acid over a silanol. If the attachment had occurred between the silanol and amine functionalization, the particles would be interacting at the non-gold-coated portion of the SiO_2 particle. The size difference of the PS and SiO_2 particles is further evidence that the desired complementary binding reaction occurred.